

## Site-Directed Mutagenesis of the 19-Kilodalton Lipoprotein Antigen Reveals No Essential Role for the Protein in the Growth and Virulence of *Mycobacterium intracellulare*

ESHWAR MAHENTHIRALINGAM,<sup>1,2,3</sup> BRITT-INGER MARKLUND,<sup>4</sup> LUCY A. BROOKS,<sup>1,2,3</sup>  
DEBBIE A. SMITH,<sup>5</sup> GREGORY J. BANCROFT,<sup>5</sup> AND RICHARD W. STOKES<sup>1,2,3,6\*</sup>

Division of Infectious and Immunological Diseases, B.C. Children's Hospital,<sup>1</sup> Canadian Bacterial Diseases Network,<sup>2</sup>  
and Departments of Paediatrics<sup>3</sup> and Pathology,<sup>6</sup> University of British Columbia, Vancouver, Canada;  
Department of Microbiology, Umeå University, Umeå, Sweden<sup>4</sup>; and Immunology Unit,  
Department of Infectious and Tropical Disease, London School of  
Hygiene and Tropical Medicine, London, United Kingdom<sup>5</sup>

Received 7 November 1997/Returned for modification 31 March 1998/Accepted 11 May 1998

**The mycobacterial 19-kilodalton antigen (19Ag) is a highly expressed, surface-associated glycolipoprotein which is immunodominant in infected patients and has little homology with other known proteins. To investigate the pathogenic significance of the 19Ag, site-directed mutagenesis of the *Mycobacterium intracellulare* 19Ag gene was carried out by using a suicide vector-based strategy. Allelic replacement of the 19Ag gene of a mouse-avirulent *M. intracellulare* strain, 1403, was achieved by double-crossover homologous recombination with a gentamicin resistance gene-mutated allele. Unfortunately, an isogenic 19Ag was not achievable in the mouse-virulent strain, D673. However, a 19Ag mutant was successfully constructed in *M. intracellulare* FM1, a chemically mutagenized derivative of strain D673. FM1 was more amenable to genetic manipulation and susceptible to site-directed mutagenesis of the 19Ag gene yet retained the virulent phenotype of the parental strain. No deleterious effects of 19Ag gene mutation were observed during *in vitro* growth of *M. intracellulare*. Virulence assessment of the isogenic 19Ag mutants in a mouse infection model demonstrated that the antigen plays no essential role in the growth of *M. intracellulare* *in vivo*. Site-directed mutagenesis of the 19Ag gene demonstrated that it plays no essential role in growth and pathogenicity of *M. intracellulare*; however, the exact nature of its biological function remains unknown.**

The genus *Mycobacterium* includes a number of pathogenic species. *Mycobacterium tuberculosis* and *M. leprae* are major causes of infectious disease worldwide (45), and *M. avium* and *M. intracellulare* (members of the *M. avium*-complex [MAC]) are opportunistic pathogens associated with infection in vulnerable hosts such as patients with AIDS (15, 22). The need to develop new and improved therapeutics and vaccines for these organisms has led to the genetic characterization of many mycobacterial antigens, and several highly conserved protein families have been identified (reviewed in reference 44). The 19-kDa antigen, 19Ag (34), is a member of a highly immunogenic family of surface-associated mycobacterial lipoproteins (23, 43). Within the *M. tuberculosis* complex, the 19Ag gene was found to be invariable (4, 13); the 19Ag genes of *M. avium* (8) and *M. intracellulare* (8, 29), in contrast, have a high degree of amino acid similarity and exhibit approximately 75% amino acid identity with the *M. tuberculosis* complex antigen. Southern hybridization analysis with 19Ag gene probes has demonstrated that several other species, including *M. asiaticum*, *M. phlei* (29), *M. kansasii*, *M. paratuberculosis*, and *M. scrofulaceum* (19), may also possess a homologous antigen, but there are currently no reports of proteins related to the 19Ag in other bacterial genera. Recent biochemical analysis of the 19Ag of *M. tuberculosis* has shown it to be one of a small number of eubacterial proteins which are glycosylated (20).

Despite its conservation among several pathogenic and non-pathogenic mycobacterial species, its consistent immunodominance in infected patients and animals, and its unique post-translational modifications, the biological function of the 19Ag remains unknown.

For most bacteria, directed mutation of a gene is a standard strategy to define the function and pathogenic significance of the gene product. However, to date, only a limited number of mycobacterial genes have been disrupted by directed mutagenesis (reviewed in reference 28). Directed mutation by homologous recombination of DNA was first achieved in fast-growing mycobacterial species; Husson et al. (21) used a suicide vector approach to accomplish allelic replacement of the *pyrF* gene of *M. smegmatis*. Several other *M. smegmatis* genes have now been successfully mutated by using this basic suicide vector strategy (reviewed in reference 28), and improved systems that use a positive-negative double selection (38) or a counterselectable marker (32) to select for allelic exchange by homologous recombination have been described. Initial studies of slow-growing mycobacteria indicated that site-directed mutagenesis by a suicide vector approach may be problematic due to the high frequency of illegitimate recombination of DNA (1, 24). However, subsequent studies with *M. bovis* BCG (30) and *M. intracellulare* (27) demonstrated that allelic replacement of genes in slow-growing mycobacterial species was possible by homologous recombination of DNA. Only a small number of target genes in slow-growing mycobacteria have now been disrupted by directed mutagenesis. These include the *ureC* gene (35) and the mycocerosic acid synthase gene of *M. bovis* BCG (5) and the *leuD* gene of *M. tuberculosis* (6). Isolation of genetically defined mycobacterial mutants not only

\* Corresponding author. Mailing address: Div. of Infectious and Immunological Diseases, Dept. of Paediatrics, Univ. of British Columbia, Rm. 304, The Research Institute, 950 West 28th Ave., Vancouver, B.C., Canada V5Z 4H4. Phone: (604) 875-2466. Fax: (604) 875-2226. E-mail: rstokes@cbdn.ca.

TABLE 1. Bacterial strains and plasmids used in this study

Strain or plasmid	Parental strain or plasmid	Relevant characteristic(s)	Source or reference
<i>E. coli</i>			
DH5 $\alpha$ F'		F' deoR <i>thi-1 endA1 hsdR17</i> ( $r_K^- m_K^+$ ) <i>supE44</i> $\lambda$ - <i>gyrA96 recA1 relA1</i> $\Delta$ ( <i>lacLZYA-argF</i> ) <i>U169</i> $\phi$ 80 <i>dlac</i> ( $\Delta$ <i>lacZ</i> ) <i>M15</i>	Gibco-BRL, Burlington, Ontario, Canada
XL1-Blue-MRF'		$\Delta$ ( <i>mcrA</i> ) <i>183</i> $\Delta$ ( <i>mcrCB-hsdSMR-mrr</i> ) <i>173 endA1 supE44 thi-1 recA1 gyrA96 relA1 lac</i> [F' <i>proAB lacI<sup>q</sup>Z</i> $\Delta$ <i>M15 Tn10</i> (Tet <sup>r</sup> )]	Stratagene Inc., La Jolla, Calif.
<i>M. intracellulare</i>			
1403 (ATCC 35716)		Smooth, domed, opaque, chromagenic morphology; mouse avirulent	Trudeau Mycobacterial Culture Collection 3
D673		Smooth, flat, transparent morphology; mouse virulent	Trudeau Mycobacterial Culture Collection 14
EM23	1403	19Ag:: <i>aacC1</i> , Gm <sup>r</sup> (1403 19Ag mutant)	This work
EM24	EM23	EM23::p19K9, Gm <sup>r</sup> Hy <sup>r</sup> (1403 complemented mutant)	This work
EM25	EM23	EM23::pUC-HY-INT, Gm <sup>r</sup> Hy <sup>r</sup> (1403 mutant vector control)	This work
FM1	D673	D673 NTG mutant, flat matt, crenate morphology, mouse virulent	This work
EM32	FM1	19Ag:: <i>aacC1</i> , Gm <sup>r</sup> (FM1 19Ag mutant)	This work
EM33	EM32	EM32::pUC-HY-INT, Gm <sup>r</sup> Hy <sup>r</sup> (mutant vector control)	This work
EM34	EM32	EM32::p19K9, Gm <sup>r</sup> Hy <sup>r</sup> (complemented mutant)	This work
Plasmids			
pUC18		Cloning vector	Laboratory collection
pUC-GM		Gm <sup>r</sup> cassette ( <i>aacC1</i> )	40
pMH94		Mycobacteriophage L5 integrase base vector	26
pYUB412		Integrative cosmid shuttle vector	31
pUC-HY	pUC-GM	1.6-kb Hy <sup>r</sup> gene cassette cloned into vector base of pUC-GM	This work
pUC-HY-INT	pUC-HY	Harbors 3.757-kb <i>HindIII</i> -excisable Hy <sup>r</sup> -L5 integrase cassette	This work
pUC-GM-INT	pUC-GM	Harbors 3.008-kb <i>HindIII</i> -excisable Gm <sup>r</sup> -L5 integrase cassette	This work
p19K4	pUC18	6.2-kb BamHI-EcoRI 19Ag-encoding locus from strain D673	This work
p19K5	p19K4	Suicide vector, 19Ag:: <i>aacC1</i> , 19Ag ORF interrupted at <i>A</i> / <i>f</i> III site	This work
p19K8	pUC18	1.0-kb <i>SalI</i> fragment carrying 19Ag ORF from strain D673	This work
p19K9	p19K8	p19K8 carrying HY-L5 integrase cassette within the single <i>HindIII</i> site of the vector; restores 19Ag expression to EM23 and EM32	This work

enables the biological role of proteins to be studied but also allows their contribution to pathogenesis to be assessed in appropriate animal models. Reyrat et al. (36) examined the growth of their isogenic *ureC* mutant of *M. bovis* BCG in mice and found that the absence of urease did not significantly alter the persistence of BCG in vivo. Improved methods for site-directed mutagenesis in slow-growing mycobacteria are being developed (7, 32) and should lead to a more widespread characterization of the pathogenic significance of characterized mycobacterial genes.

Directed mutagenesis of the 19Ag of *M. intracellulare* was undertaken, in part, to confirm that the novel observation of homologous recombination in *M. intracellulare*, identified in a model target gene system (27), could be applied to a true mycobacterial gene. However, the primary objective of our study was to explore the role of the 19Ag in virulence. In our model system, gene replacement of a chromosomally integrated gentamicin resistance (Gm<sup>r</sup>) gene (*aacC1*) was achieved by using a suicide vector carrying a copy of *aacC1* interrupted with a kanamycin resistance (Kan<sup>r</sup>) cassette. Characterization of the Kan<sup>r</sup> plasmid integrants demonstrated that only single-crossover homologous recombination events had occurred. Subsequent growth of one recombinant clone and extensive screening for gentamicin-sensitive colonies led to the isolation of a derivative in which complete allelic replacement of *aacC1* had taken place (27). This proof of principle suggested that homologous recombination could be used to disrupt defined genes in *M. intracellulare*, and the 19Ag was chosen as one target because it is highly conserved (8) and immunodominant (23) in several slow-growing pathogenic species, because its DNA se-

quence was available (8, 29), and because of its unique association with mycobacteria and a lack of homology with other known proteins. Lathigra et al. (25) found that two of nine *M. tuberculosis* isolates examined lacked expression of the 19Ag and suggested that the antigen may play a role in virulence after examining the growth kinetics of a 19Ag-deficient strain and its complemented counterpart in mice. In the study presented here, isogenic 19Ag mutants of two *M. intracellulare* strains were constructed by site-directed mutagenesis and used to examine the role for the 19Ag in bacterial growth and virulence. The *M. intracellulare* strain, 1403, in which homologous recombination had been originally demonstrated (27), is avirulent in mouse models of MAC infection (10, 12). Here we describe the construction of 19Ag mutants both in this avirulent strain background and in an additional *M. intracellulare* strain, FM1, an experimental derivative of the mouse-virulent strain D673 (14). A basic suicide vector approach was applied, and complete allelic replacement was achieved in a single step by a double-crossover homologous recombination event. Site-directed mutagenesis of the *M. intracellulare* 19Ag gene, complementation with novel vector constructs and virulence assessment of the resulting isogenic 19Ag mutants are described.

#### MATERIALS AND METHODS

**Bacterial strains and growth.** *M. intracellulare* strains used in this study are shown in Table 1. Mycobacteria were grown on Middlebrook 7H10 agar or in 7H9 broth containing oleic acid-albumin-dextrose complex without added catalase. Modified Proskauer and Beck minimal medium was also used for growth of mycobacterial strains (3). All liquid growth media contained 0.05% Tween 80 to prevent clumping of bacteria. Phosphate-limited minimal medium was prepared by using a Proskauer and Beck medium base, except that the potassium phos-

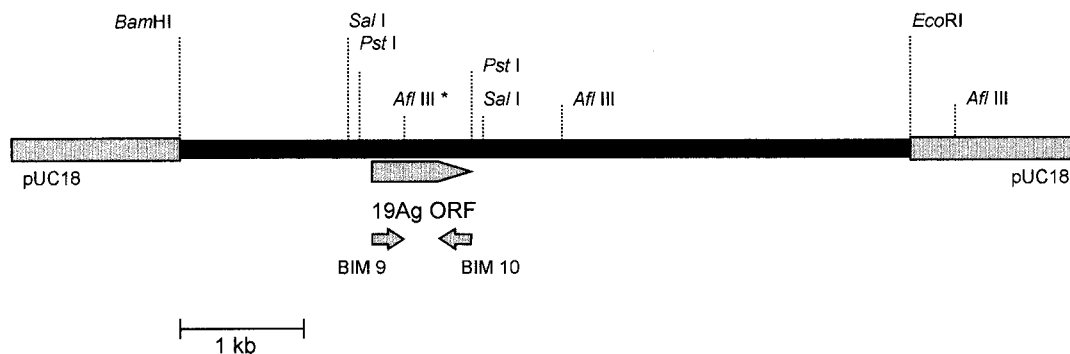


FIG. 1. Partial restriction map of plasmid p19K4. The 6.2-kb *Bam*HI-*Eco*RI insert of p19K4 encoding the 19Ag gene locus of *M. intracellulare* D673 is illustrated diagrammatically. Pertinent restriction sites, the 19Ag gene ORF, and PCR primer binding sites are shown. The site at which the 19Ag gene ORF was disrupted by insertion of the *Gm*<sup>r</sup> cassette of pUC-GM is indicated (*Afl*III\*).

phate buffer was replaced by 10 mM HEPES, and bovine serum albumin (5 mg/ml) and glucose (5 mg/ml) were added. Mycobacterial growth rate in liquid media was monitored by recording a culture's optical density at 600 nm.

Gentamicin (5 µg/ml) and hygromycin B (50 µg/ml) were added to mycobacterial growth media as required. Subcloning of DNA was performed in *Escherichia coli* DH5αF' and XL1-Blue-MRF' (Table 1), and *E. coli* strains were grown in standard nutrient media supplemented with the appropriate antibiotics as described elsewhere (37).

**Preparation of DNA and recombinant DNA techniques.** Plasmid DNA for electroporation of *M. intracellulare* was prepared from *E. coli* strains by alkaline lysis (37), and standard cloning and Southern hybridization procedures were used for all manipulations of DNA (37). High-molecular-weight *M. intracellulare* chromosomal DNA was prepared as described elsewhere (27). Chromosomal DNA miniprep procedures were performed on mycobacteria as described previously (26), using a modified lysis buffer (50 mM Tris-HCl [pH 8], 50 mM EDTA [pH 8], 1% sodium dodecyl sulfate [SDS]) and 2-min disruption with 0.1-mm-diameter zirconium beads on a reciprocal shaking device (Mini Bead-beater; Biospec Products, Bartlesville, Okla.).

**Subcloning of *M. intracellulare* D673 19Ag gene.** PCR primers were designed from the DNA sequence of the 19Ag gene of *M. intracellulare* serotype 18 (8; GenBank accession no. L12238). The forward primer used was BIM-9 (5'-AA CAAGTCGGGAACGAGCG-3', corresponding to base positions 76 to 94 within the 19Ag gene open reading frame [ORF]); the reverse primer was BIM-10 (5'-TTGATTTTCGAACGGTTTG-3', corresponding to positions 470 to 453 within the antigen ORF). PCR amplification was performed under standard reaction conditions, using 30 cycles of 94°C for 1 min, 63°C for 1 min, and 72°C for 2 min. The resulting 395-bp product was labeled with 50 µCi of [<sup>32</sup>P]dGTP (Amersham, Oakville, Ontario, Canada), using a randomly primed DNA labeling kit (Boehringer Mannheim, Montreal, Quebec, Canada). Using this probe, we identified cosmids carrying the 19Ag gene of *M. intracellulare* D673 from an *M. intracellulare* library constructed in the vector pJB8 (27a) by Southern hybridization under stringent conditions. A 6.2-kb *Bam*HI-*Eco*RI restriction fragment bearing the antigen was subcloned from one of these cosmids into pUC18, creating plasmid p19K4 (Table 1).

**Suicide vector construction.** Plasmid p19K4 (Table 1) and the *M. intracellulare* 19Ag gene sequence were each examined for restriction sites which could facilitate 19Ag gene ORF disruption. A single restriction site for the endonuclease *Afl*III was identified 185 bp into the 489-bp 19Ag gene sequence. Restriction mapping of p19K4 revealed a second *Afl*III site, approximately 0.9 kb downstream from the site within the 19Ag gene ORF (Fig. 1); in addition, a single *Afl*III site was present in pUC18. The *Afl*III site of pUC18 was deleted after restriction digestion by Klenow DNA polymerase reaction (37) followed by religation, and the 6.2-kb *Bam*HI-*Eco*RI fragment of p19K4 was subcloned into this modified pUC18 vector to create plasmid p19K4A. Plasmid p19K4A was linearized by partial digestion with *Afl*III, and blunt ends were created by Klenow DNA polymerase reaction (37). An 855-bp *Sma*I-generated DNA fragment encoding the *Gm*<sup>r</sup> gene, *aac*CI, from pUC-GM (40) was then ligated into partially cut p19K4A.1, and the products were transformed into *E. coli* DH5αF'. *Gm*<sup>r</sup> transformants were screened by PCR to identify clones which contained the 19Ag gene ORF interrupted with the *Gm*<sup>r</sup> cassette (Fig. 2). Plasmid genotype was confirmed by digestion with *Afl*III, and one clone with a correctly interrupted 19Ag gene ORF and unaltered downstream *Afl*III site (Fig. 1) was designated plasmid p19K5, the 19Ag gene suicide mutagenesis vector (Table 1).

**Construction of mycobacterial cloning cassettes.** Two resistance gene cassettes were used for antibiotic selection in mycobacteria: the *Gm*<sup>r</sup> gene cassette from pUC-GM (40) and a hygromycin B resistance (*Hy*<sup>r</sup>) gene cassette constructed in the same vector base as pUC-GM. The *Hy*<sup>r</sup> gene cassette was constructed as follows. A 1,596-bp fragment encoding the hygromycin B phosphotransferase gene (46) of the integrative cosmid pYUB412 (31) was subcloned by PCR

amplification using primers HYG-1 (5'-TTGGTACCGCCGTCGGCCGCCCC-3') and HYG-2 (5'-GGGGTACCAAGCCCTCGGCGACG-3'), each of which possessed 5' ends encoding a *Kpn*I restriction site. The *Kpn*I-restricted *Hy*<sup>r</sup> gene amplification product was subcloned into the vector base of pUC-GM derived by digestion with *Kpn*I. The resulting plasmid, pUC-HY (Table 1), liberated an intact 1.6-kb *Hy*<sup>r</sup> cassette when digested with the enzymes *Kpn*I, *Bam*HI, *Xba*I, *Pst*I, and *Hind*III.

Construction of the positive-selection L5 integrase cassettes was carried out as follows. The 2.089-kb *Sal*I fragment of pMH94 (Table 1) encoding complete integrase activity (26) was cloned into pUC-HY and pUC-GM, both of which had been linearized by partial digestion with *Sal*I. After restriction mapping of the resultant clones, two plasmids were selected: pUC-HY-INT (Table 1), which liberated a 3.757-kb *Hy*<sup>r</sup>-integrase cassette when digested with *Hind*III, and pUC-GM-INT (Table 1), which liberated a 3.008-kb *Gm*<sup>r</sup>-integrase cassette when restricted with *Hind*III. The DNA sequences of pUC-HY, pUC-GM-INT, and pUC-HY-INT were assembled from the published sequences of the vectors (40) and the genes (26, 40, 46) used in their construction.

**Chemical mutagenesis.** *M. intracellulare* D673 was subjected to chemical mutagenesis with *N*-methyl-*N'*-nitro-*N*-nitrosoguanidine (NTG) exactly as described previously (9). Briefly, mycobacteria were grown to late log phase in 100 ml of Proskauer and Beck minimal medium containing 0.05% Tween 80, harvested, and resuspended in 20 ml of 0.2 M KH<sub>2</sub>PO<sub>4</sub> (pH 6.3) buffer containing 0.05% Tween 80 (PBST) and 0.5 mg of NTG per ml. After incubation at 37°C for 1 h, the bacteria were washed four times in PBST and then left to recover in 100 ml of 7H9 broth at 37°C for 24 h. The resulting mutant bank was then frozen in aliquots at -70°C. A portion of the D673 NTG bank was then plated to single colonies on 7H10 agar, and approximately 10,000 mutants were screened for alterations in colony type after 14 days of growth at 37°C. *M. intracellulare* FM1 (Table 1), which possessed a flat matt, crenate colony type, was one of the morphologically altered mutants isolated from this screen.

**Directed mutagenesis of *M. intracellulare*.** Electrocompetent mycobacteria were prepared and electroporated as previously described (27) except that all procedures were performed at room temperature. Approximately 1 to 2 µg of plasmid p19K5 was electroporated into *M. intracellulare* 1403 and FM1. After 24 h of recovery in 7H9 medium, bacteria were plated onto 7H10 agar supplemented with gentamicin and incubated at 37°C for 10 to 14 days. *Gm*<sup>r</sup> transformants were then inoculated individually into 3 ml of 7H9 broth contained in a 13-ml culture tube and grown at 37°C for 7 days. One milliliter of each resulting culture was frozen for storage, and the remaining 2 ml of bacterial growth was harvested by centrifugation. Chromosomal DNA was then isolated from the bacterial pellet by the miniprep procedure and analyzed by PCR with primers BIM-9 and BIM-10 for determination of the type of DNA recombination event that had taken place with plasmid p19K5 (Fig. 2).

**Protein extraction.** Mycobacterial protein extracts were prepared from 200-ml cultures of bacteria grown to late log phase in minimal media. Bacteria were harvested by centrifugation and washed twice in PBST. All subsequent procedures were then performed on ice. Pellets were resuspended in 1 ml of PBS containing 5 mM EDTA (pH 8) and 1 mM phenylmethylsulfonyl fluoride and then placed in a 2-ml screw-cap tube containing 1 ml of 0.1-mm-diameter zirconium beads. Bacteria were disrupted by a 5-min pulse on a reciprocal shaking device (Mini Bead-beater; Biospec Products), and cell extracts were generated by removal of cellular debris by high-speed centrifugation. After sterilization by filtration through a 0.22-µm-pore-size filter (Millipore, Bedford, Mass.), the protein concentration of a small portion of each extract was determined by bicinchoninic acid reaction (Sigma Chemical Co., Mississauga, Ontario, Canada), and extracts were frozen at -20°C for storage.

**Western blot analysis.** A polyclonal rabbit antiserum was raised against purified recombinant *M. tuberculosis* 19Ag (rTB19Ag) (16) by standard subcutaneous immunization of two full-grown female New Zealand White rabbits (18). Purified

*M. tuberculosis* 19Ag was kindly provided by Christiane Abou-Zeid, Imperial College of Science and Technology, University of London, St. Mary's Hospital, London, England. Each rabbit was immunized with 200 µg of rTB19Ag in incomplete Freund's adjuvant (Gibco-BRL). A primary and a secondary boost, each with 100 µg of 19Ag in Freund's incomplete adjuvant, were performed 5 and 10 weeks, respectively, after the initial immunization. Antiserum was prepared from each rabbit 12 days after the secondary boost, and the sera were pooled. The titer of the pooled serum was determined by enzyme-linked immunosorbent assay (18) and was approximately 1:80,000 when tested against 100 ng of rTB19Ag per well.

Mycobacterial protein extracts were fractionated by standard SDS-polyacrylamide gel electrophoresis (PAGE) (37) in 15% acrylamide gels and transferred to nitrocellulose by wet transfer (Mini Trans Blot; Bio-Rad Laboratories, Mississauga, Ontario, Canada). Standard immunoblot techniques were used (18), and blotted proteins were probed with a 1:5,000 dilution of the 19Ag rabbit antiserum. Blots were developed by incubation with a 1:1,000 dilution of alkaline phosphatase-conjugated goat anti-rabbit antibody (Kirkegaard & Perry Laboratories Inc., Gaithersburg, Md.) and subsequent bromochloroindolylphosphate-nitroblue tetrazolium substrate reaction (18).

**Mouse infection.** Intravenous infection of BALB/c mice (11) and SCID mice (17) with *M. intracellulare* strains was carried out as described previously. The infection doses were approximately  $1 \times 10^6$  and  $5 \times 10^5$  viable *M. intracellulare* for BALB/c mice and SCID mice, respectively. Three mice were assessed per time point, and the bacterial loads in liver, spleen, and lung homogenates were quantitated by serial dilution on 7H10 agar followed by culture at 37°C for 10 to 14 days (11). Statistical analysis of the mouse infection data was performed by using Student's *t* test with independent means;  $P < 0.05$  was considered to be significantly different.

**Nucleotide sequence accession numbers.** The DNA sequences of pUC-HY, pUC-GM-INT, and pUC-HY-INT have been submitted to GenBank and assigned accession no. AF025747, AF025392, and AF025746, respectively.

## RESULTS

**Suicide vector design.** The published 19Ag gene sequence of *M. intracellulare* serotype 18 (8) was used to design PCR primers (BIM-9 and BIM-10) which were used to amplify a 395-bp portion of the *M. intracellulare* D673 19Ag gene. Using this PCR probe, seven 19Ag gene-positive cosmids were identified in an *M. intracellulare* D673 library, and a 6.2-kb *Bam*HI-*Eco*RI DNA fragment encoding the 19Ag gene was subcloned from one of them into pUC18. The resulting plasmid, p19K4 (Table 1), was mapped by digestion with restriction enzymes in order to identify potential sites for gene disruption. A partial restriction map of p19K4 is shown in Fig. 1. To disrupt the 19Ag gene borne on p19K4, an 855-bp *Gm*<sup>r</sup> cassette from pUC-GM (40) was inserted at the single *Afl*III restriction site within the 19Ag gene ORF (Fig. 1), thus creating the suicide vector p19K5 (Table 1). Plasmid p19K5 did not contain a mycobacterial origin of replication because it was based on the *E. coli* cloning vector pUC18. The binding sites for PCR primers BIM-9 and BIM-10 flanked the site of 19Ag gene disruption (Fig. 1).

**Directed mutagenesis of the *M. intracellulare* 19Ag gene.** Directed mutagenesis of the mouse-avirulent *M. intracellulare* strain 1403 in which gene replacement by homologous recombination had been successfully carried out (27) was attempted first. Electroporation of 1403 with 1 µg of plasmid p19K5 resulted in the isolation of 12 *Gm*<sup>r</sup> transformants. Four additional electroporations using p19K5 resulted in between 8 and 15 *Gm*<sup>r</sup> transformants per electroporation. PCR with primers BIM-9 and BIM-10 was used as a rapid screen for the type of recombination undergone with the suicide vector. Three PCR amplification patterns were observed among the *Gm*<sup>r</sup> transformants (Fig. 2A): first, the wild-type 395-bp product, indicative of either spontaneous *Gm*<sup>r</sup> clones or clones in which illegitimate integration of p19K5 had resulted in the loss of one or other suicide vector-borne primer binding sites; second, a single 1,250-bp amplification product indicative of gene replacement by the mutant allele of p19K5; and third, 395- and 1,250-bp PCR products indicative of either (i) clones having undergone single-crossover homologous recombination resulting in

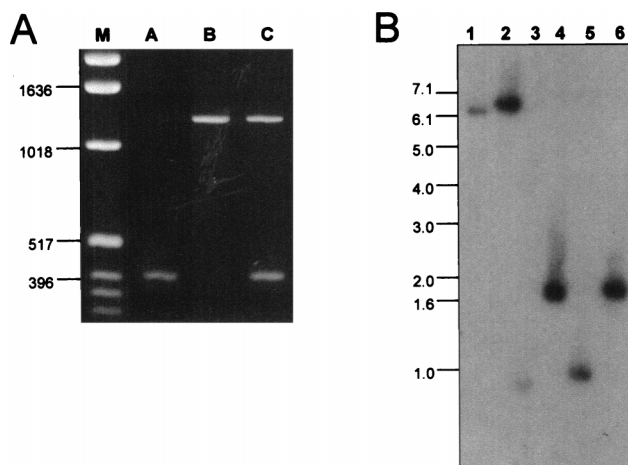


FIG. 2. PCR and Southern hybridization screening of putative 19Ag mutants. (A) PCR amplification patterns generated with primers BIM-9 and BIM-10. Lane M, molecular size markers (sizes in base pairs are indicated); lane A, 395-bp product amplified from *M. intracellulare* 19Ag gene; lane B, 1,250-bp product amplified from putative 19Ag mutants; lane C, 395- and 1,250-bp products amplified from transformants which had undergone either single-crossover recombination or illegitimate recombination with p19K5. (B) Southern hybridization analysis of *M. intracellulare* chromosomal DNA extracted from strain 1403 and its 19Ag mutant, strain EM23. DNAs and restriction digests were as follows: lane 1, 1403, *Bam*HI-*Eco*RI; lane 2, EM23, *Bam*HI-*Eco*RI; lane 3, 1403, *Pst*I; lane 4, EM23, *Pst*I; lane 5, 1403, *Sal*I; lane 6, EM23, *Sal*I. The Southern blot was probed with the radiolabeled 395-bp 19Ag gene PCR probe (see panel A) under the conditions described in Materials and Methods. Positions of molecular size standards are indicated on the left of panel B (sizes in kilobases).

plasmid integrants carrying both wild-type and mutant 19Ag gene alleles or (ii) illegitimate insertion of p19K5. The 12 initial *Gm*<sup>r</sup> transformants were screened by PCR, and 11 were found to possess amplification patterns indicating apparent single-crossover or illegitimate recombination with p19K5 (Fig. 2A). The remaining clone possessed a PCR amplification pattern with only the mutant 19Ag gene allele detected (Fig. 2A), indicative of a putative 19Ag mutant and suggesting that complete allelic replacement of the 19Ag gene had taken place. The putative 1403 19Ag mutant was designated *M. intracellulare* EM23 (Table 1) and set aside for characterization.

Repeated electroporation of mouse-avirulent *M. intracellulare* D673 with p19K5 resulted in the isolation of large numbers of spontaneous *Gm*<sup>r</sup> clones, none of which appeared to have undergone recombination with the suicide plasmid when screened by PCR (data not shown).

**Isolation of 19Ag mutant of a mouse-avirulent *M. intracellulare* strain.** Because of the failure to obtain a 19Ag mutant of strain D673, an alternative mouse-avirulent *M. intracellulare* strain, amenable to genetic manipulation, was required to assess the role of the 19Ag in virulence. *M. intracellulare* FM1, a derivative of strain D673, had been obtained by chemical mutagenesis of strain D673 with NTG (9). Strain D673 NTG mutant banks were screened for alterations in colony morphology, a phenomenon associated with virulence phenotype in MAC (39). This screen resulted in the isolation of strain FM1, which possessed a stable flat, matt, crenate morphology, in contrast to strain D673, its parental isolate, which possessed a flat, transparent, smooth colony morphology (14). Unlike the parental D673, FM1 was susceptible to antibiotics and readily transformable with L5 integrase-based vectors such as pYUB412 (Table 1), yet like D673, it is virulent in a mouse model of infection (see Fig. 6). Strain FM1 was found to be susceptible to directed mutagenesis with p19K5 in a fashion

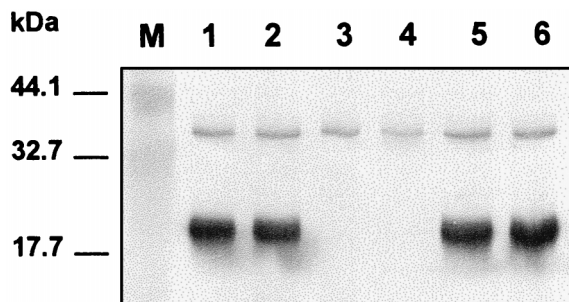


FIG. 3. Analysis of 19Ag expression in *M. intracellulare*. Protein extracts of *M. intracellulare* (approximately 20  $\mu$ g of total protein) were separated by SDS-PAGE and probed by Western blotting with rabbit polyclonal antiserum raised against purified recombinant *M. tuberculosis* 19Ag. Lane M, molecular size markers (sizes are shown on the left); lane 1, strain D673; lane 2, strain FM1; lane 3, strain EM32 (19Ag mutant); lane 4, strain EM33 (19Ag mutant vector control); lane 5, strain EM34 (complemented mutant); lane 6, strain 1403.

analogous to that with *M. intracellulare* 1403. A single electroporation of strain FM1 with 2  $\mu$ g of DNA resulted in the isolation of 29 Gm<sup>r</sup> transformants, of which 2 possessed the PCR amplification patterns characteristic of a 19Ag mutant (Fig. 2A). One of these putative mutants, strain EM32 (Table 1), was further characterized.

**Southern hybridization analysis.** To confirm the results of the PCR screen, the putative 1403 and FM1 19Ag mutants were examined by Southern hybridization for the presence of the mutated 19Ag gene allele. Southern hybridization analysis of the 19Ag gene locus of *M. intracellulare* 1403 and its isogenic 19Ag mutant, strain EM23, is shown in Fig. 2B. Restriction fragment length polymorphism (RFLP) analysis was carried out on the entire 6.2-kb *Bam*HI-*Eco*RI region and on smaller DNA fragments being liberated by digestion with the enzymes *Pst*I and *Sal*I, which possess recognition sites flanking the 19Ag gene ORF (Fig. 1). In each case, the RFLP of strain EM23 demonstrated a 0.85-kb increase in size over the parental 1403 RFLP correlating to the presence of the *aac*CI-mutated 19Ag gene allele (Fig. 2B). The wild-type 19Ag gene and the presence of pUC18 DNA from the suicide vector were not detected in strain EM23. These data indicated that a one-step double-crossover homologous recombination event had taken place in *M. intracellulare* EM23 which resulted in complete allelic replacement of the 19Ag gene with the *aac*CI-interrupted 19Ag gene allele of plasmid p19K5. Southern hybridization of strain EM32, the isogenic 19Ag mutant of *M. intracellulare* FM1 (Table 1), also demonstrated the presence of only the mutated 19Ag gene allele (data not shown), confirming complete 19Ag gene replacement by allelic exchange.

**Western blot analysis.** Expression of the 19Ag of *M. intracellulare* was examined by immunoblotting using a polyclonal rabbit antibody raised against purified recombinant *M. tuberculosis* 19Ag (16). SDS-PAGE-fractionated *M. intracellulare* protein extracts probed by immunoblotting with the 19Ag polyclonal antibody are shown in Fig. 3. The polyclonal sera raised against the *M. tuberculosis* 19Ag reacted strongly with the 19Ag of *M. tuberculosis* H37Rv (data not shown) and the 19Ag proteins of *M. intracellulare* 1403, D673, and FM1 (Fig. 3). The 19Ag signals obtained from 20  $\mu$ g of total protein from each of the *M. intracellulare* strains were comparable, indicating that the levels of expression of the antigen were similar in all strains (Fig. 3). Cross-reaction of the polyclonal antibody with a protein migrating at a molecular size of 38 kDa was apparent in all *M. intracellulare* (Fig. 3) and *M. tuberculosis* (data not shown) total protein extracts. Immunoblot analysis of the *M. intracel-*

*lulare* FM1 19Ag mutant EM32 (Fig. 3) and strain 1403-derived mutant EM23 (data not shown) demonstrated that expression of the 19Ag had been successfully abrogated as a result of the insertion of the Gm<sup>r</sup> cassette. The signal from the cross-reacting 38-kDa protein was unaltered in each strain (data for EM32 are shown in Fig. 3), and the total protein profile was unchanged from that of the parental strains except for the absence of the 19Ag (data not shown).

**Complementation of 19Ag mutants.** Each mutant was complemented with the wild-type 19Ag gene allele in order to restore antigen expression. Complementation was achieved as follows. A 1-kb *Sal*I fragment from p19K4 (Fig. 1), encoding the 19Ag gene with a minimum of flanking DNA, was subcloned into pUC18, creating plasmid p19K8 (Table 1). To introduce plasmid p19K8 (a ColE1 replicon [Table 1]) into *M. intracellulare*, positive-selection cloning cassettes were constructed based on the mycobacteriophage L5 integrase gene locus. The mycobacteriophage integrase catalyzes site-specific integration of DNA into the chromosomes of *M. smegmatis* and *M. tuberculosis* (26) and of *M. intracellulare* (27). A 2-kb region of pMH94 (Table 1) encoding complete integrase and attachment functions (26) was introduced into the Gm<sup>r</sup> and Hy<sup>r</sup> cassette-bearing plasmids pUC-GM (40) and pUC-HY (Table 1), respectively. The resulting plasmids, pUC-GM-INT and pUC-HY-INT (Table 1), when digested with the enzyme *Hind*III, liberated 3.089-kb Gm<sup>r</sup>-integrase and 3.757-kb Hy<sup>r</sup>-integrase cassettes, respectively. Electroporation of plasmids pUC-GM-INT and pUC-HY-INT into *M. intracellulare* 1403 resulted in transformation frequencies of approximately 10<sup>4</sup> transformants per  $\mu$ g of DNA, indicating that the presence of either cassette in ColE1-based cloning vectors could facilitate their introduction into mycobacteria.

The 3.757-kb *Hind*III Hy<sup>r</sup>-integrase cassette was introduced into p19K8 (which encoded the 19Ag gene), creating plasmid p19K9 (Table 1), which was then electroporated into the Gm<sup>r</sup> 19Ag mutants EM23 and EM32. Several thousand Hy<sup>r</sup> transformants were isolated from each electroporation, of which six of six from each strain expressed the 19Ag when analyzed by immunoblotting (data not shown). Two individual clones, EM24 (the complemented 1403 19Ag mutant [Table 1]) and EM34 (the complemented FM1 19Ag mutant [Table 1]), were set aside for further characterization. The level of 19Ag expression restored by integration of p19K9 into the chromosome of each mutant was comparable to that for the wild-type parental isolates and is shown for strain EM34 in Fig. 3. Vector control strains were also created by the introduction of pUC-HY-INT into EM23 and EM32, resulting in the isolation of strains EM25 and EM33 (Table 1). Both vector control strains lacked expression of the 19Ag; an immunoblot of strain EM33, the FM1 19Ag mutant-derived vector control, is shown in Fig. 3. The Gm<sup>r</sup>-integrase cassette of pUC-GM-INT was also used to successfully introduce plasmid p19K8, carrying the 19Ag gene from strain D673, into strain 1403 in a control experiment (data not shown).

**Growth of *M. intracellulare* 19Ag mutants in vitro.** The wild-type *M. intracellulare* strains and their isogenic 19Ag mutant, complemented mutant, and vector control derivatives demonstrated the following growth characteristics in vitro. Parental growth morphology, smooth domed for 1403 and flat matt for FM1 (Table 1), was retained by all derivative constructs after growth on Middlebrook 7H10 agar. In nutrient-rich Middlebrook 7H9 broth, all strains grew well and at similar rates, requiring approximately 12 days to reach stationary phase (data not shown). The 19Ag gene mutation of strains EM23 and EM32 (Table 1) remained stable during prolonged growth without Gm<sup>r</sup> selection, and the complemented *M. intracellulare*

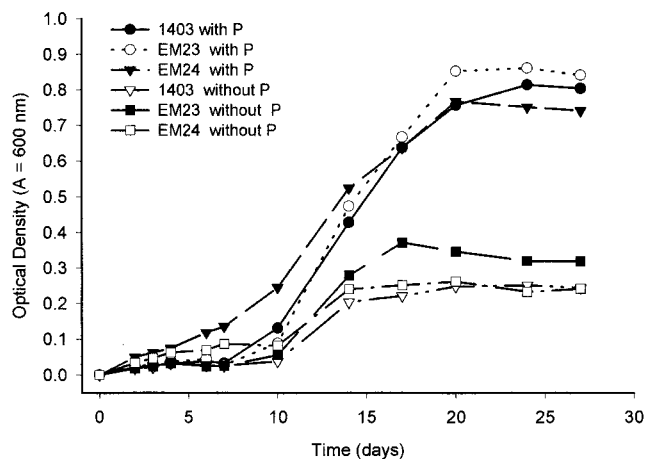


FIG. 4. Growth of *M. intracellulare* 1403, EM23, and EM24 in minimal media with and without phosphate (P). The optical density of bacterial cultures is plotted against the time of growth (days) for each strain and growth medium indicated in the key.

19Ag mutants, strains EM24 and EM34 (Table 1), maintained their restored 19Ag expression levels in the absence of Hy<sup>r</sup> selection (data not shown).

Andersen and Brennan (2) postulated that the *M. tuberculosis* 19Ag may play a role in phosphate transport because its expression is upregulated under phosphate-limited growth conditions. To explore this hypothesis in our *M. intracellulare* model, strains 1403, EM23 (19Ag mutant), and EM24 (complemented mutant) were grown with and without phosphate in Proskauer and Beck minimal experimental media. Approximately  $10^6$  viable bacteria were inoculated into 100 ml of each minimal medium, and growth was monitored by culture optical density; the resulting growth curves are shown in Fig. 4. In minimal media with phosphate, 1403, EM23, and EM24 grew well, reaching stationary phase in approximately 20 days (Fig. 4). Without phosphate, all three strains grew very poorly, reaching approximately one-third of the density of cultures grown in the presence of phosphate before growth ceased between 15 and 20 days (Fig. 4). Similar results were obtained with strain FM1 and its isogenic 19Ag mutant derivatives (data not shown). Thus, mutation of the 19Ag gene of *M. intracellulare* did not appear to compromise its growth in vitro.

**Growth of the *M. intracellulare* 19Ag mutants in vivo.** The survival of *M. intracellulare* 1403 and its isogenic 19Ag mutant, EM23, was initially assessed with BALB/c mice following intravenous inoculation. Both strains were progressively eliminated at the same rate from the spleens, livers, and lungs of the mice, resulting in negligible bacterial counts being detected after 35 days of infection (data not shown). Unfortunately, *M. intracellulare* 1403 is avirulent in healthy mice (10, 12) (see Fig. 6), which compromised our ability to detect any deleterious effect of the 19Ag mutation on the survival of 1403 in BALB/c mice. We therefore tested strains 1403 and EM23 in immunocompromised SCID mice, reasoning that these mice may not be able to control bacterial growth. Indeed, after intravenous inoculation, *M. intracellulare* 1403 demonstrated better persistence in the target organs of SCID mice, but it was still gradually eliminated. The survival kinetics of strain 1403 and EM23 in the spleens of SCID mice are shown in Fig. 5; there was no significant difference ( $P > 0.05$ ) in the rates at which the two strains were eliminated.

We therefore investigated the role of the 19Ag in virulence, using the mouse-virulent *M. intracellulare* strain FM1 and its isogenic 19Ag mutant, complemented mutant, and vector con-

trol derivatives (Table 1). BALB/c mice were infected intravenously with these strains and *M. intracellulare* 1403 and D673 controls. The number of bacteria surviving in the spleen after 1, 15, and 35 days of infection is shown in Fig. 6; similar results were obtained for the liver and lung (data not shown). *M. intracellulare* D673, the virulent wild-type strain from which the NTG mutant FM1 was derived, grew well in the spleens of BALB/c mice (Fig. 6A) as previously described (11). Strain FM1 grew at a slightly lower rate than the virulent control strain D673 (numbers of CFU of viable bacteria surviving in the spleen for each strain after 35 days of infection were significantly different;  $P < 0.05$ ); however, it was not rapidly eliminated like the avirulent strain *M. intracellulare* 1403 (Fig. 6A). Loss of the 19Ag did not significantly alter the rate of growth of strain FM1 (Fig. 6A;  $P > 0.05$  for comparison of day 35 spleen counts), with the numbers of both FM1 and EM32 in the spleen increasing approximately 1 log by day 35 (Fig. 6B). The FM1 derivatives carrying L5 mycobacteriophage-based integrative plasmids within their chromosome, EM33 (the 19Ag mutant vector control) and EM34 (the complemented 19Ag mutant), both demonstrated a significantly lower rate of growth than FM1 or EM32 (Fig. 6A;  $P < 0.05$  for comparison of day 35 spleen counts). After 35 days, EM33 and EM34 had increased in numbers by approximately 0.5 log, and the final growth differential between them and their parental strain, FM1, was approximately 0.5 log (Fig. 6B). Colony morphology, presence or absence of the 19Ag, antibiotic selective marker profile, and 19Ag PCR genotype were tested for all bacteria recovered after 35 days of infection and found to be the same as before inoculation into the mice (data not shown).

## DISCUSSION

We have demonstrated that successful site-directed mutagenesis of the 19Ag gene of *M. intracellulare* 1403, a mouse-avirulent isolate, can be achieved by direct double-crossover homologous recombination with a suicide vector. Allelic replacement of the 19Ag gene of a mouse-virulent *M. intracellulare* strain was also successful, but only when we used a derivative strain, FM1, isolated by chemical mutagenesis of the wild-type strain D673 with NTG. Neither of the isogenic 19Ag mutants showed any marked alteration in colony morphology

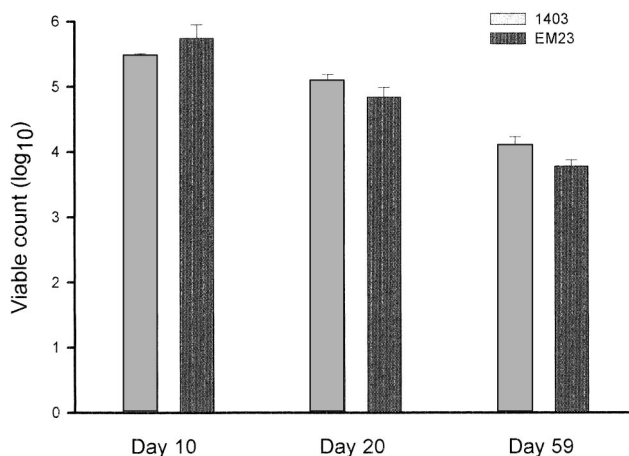


FIG. 5. Survival of *M. intracellulare* 1403 and its 19Ag mutant (EM23) in spleens of SCID mice. Numbers of viable bacteria ( $\log_{10}$ ) cultured from spleen homogenates on days 10, 20, and 59 following intravenous infection with approximately  $5 \times 10^5$  viable bacteria are shown. The mean count from each group of three mice and standard deviation are plotted for each time point.

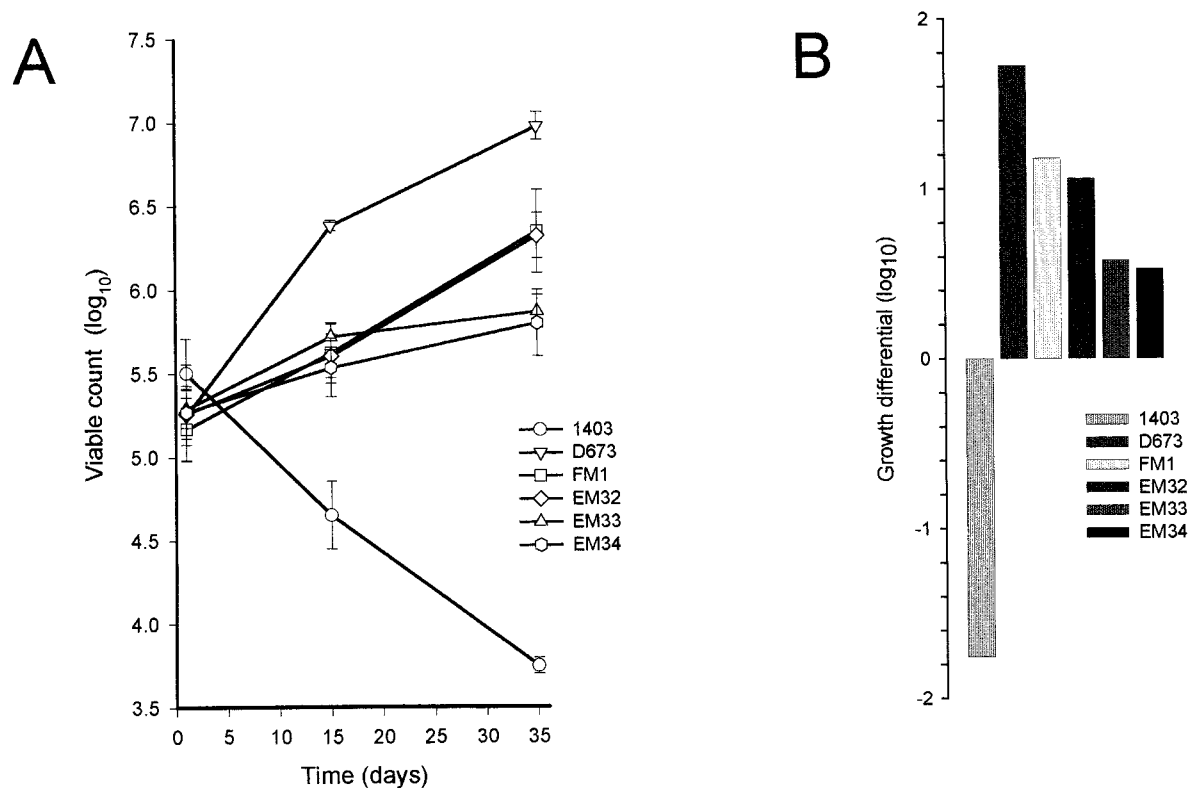


FIG. 6. Survival of *M. intracellulare* strains in spleens of BALB/c mice. (A) Numbers of viable bacteria ( $\log_{10}$ ) cultured from spleen homogenates on days 1, 15, and 35 following intravenous infection with approximately  $10^6$  viable CFU of *M. intracellulare* 1403, D673, FM1, EM32, EM33, and EM34. The mean count for each group of three mice and the standard deviation are plotted for each time point. (B) Overall  $\log_{10}$  growth differential (day 1 viable count subtracted from day 35 viable count) for each of the *M. intracellulare* strains in spleens of infected mice.

and growth in vitro. Virulence of the 19Ag mutant of strain FM1 was also unaltered when evaluated with a BALB/c mouse infection model.

Preliminary studies with *M. intracellulare* had demonstrated that allelic replacement of model target genes could be achieved by homologous recombination in this slow-growing mycobacterial species (27). In that system, only clones in which single-crossover homologous recombination events had occurred were isolated after introduction of a suicide vector (27). In the present study, in which the 19Ag gene of *M. intracellulare* was the target for site-directed mutagenesis, apparent illegitimate or single-crossover recombination events were demonstrated by a PCR screen of the transformants selected after electroporation of the suicide vector, p19K5. In addition, double-crossover homologous recombination with p19K5 had also occurred, leading to the direct isolation of 19Ag mutants in which complete allelic replacement of the 19Ag gene was subsequently confirmed by Southern hybridization. These different outcomes of a similar site-directed mutagenesis approach suggest that the type of recombination event occurring after introduction of suicide vectors into mycobacteria may also be dependent on the nature and location of the target gene locus. Nevertheless, despite the differences in DNA recombination events, each approach ultimately enabled successful allelic replacement of the respective gene target in *M. intracellulare*.

Isolation of the *M. intracellulare* D673-derived NTG mutant strain FM1 facilitated uncomplicated construction of isogenic 19Ag mutants in a mouse-virulent MAC background. The amenability of FM1 to genetic manipulation and its high-frequency DNA transformation phenotype are analogous to the

phenotype of *M. smegmatis* mc<sup>2</sup>155, the prototypic fast-growing nonpathogenic mycobacterial cloning strain (41). Snapper et al. (41) were unable to define the mutation(s) which leads to the efficient plasmid transformation phenotype of strain mc<sup>2</sup>155, and the genetic and physiological basis for its altered phenotype remain unknown. The nature of the NTG mutation suffered by strain FM1 is currently being investigated by a genetic complementation approach.

To complement the site-directed 19Ag gene mutations, novel mycobacterial cloning cassettes were constructed based on the mycobacteriophage L5 integrase (26), which to date is the sole means of obtaining stable transformants in *M. intracellulare* (27). These cassettes enable efficient introduction of DNA constructs into mycobacteria at single copy number and may prove useful for complementation of future mutants isolated by site-directed mutagenesis. Each integrase-selectable marker cassette is large (>3 kb), and excision of the cassette is limited to digestion with the enzyme *Hind*III. However, the positive selection encoded by Gm<sup>r</sup> or Hy<sup>r</sup> markers makes their introduction into a variety of *E. coli* vector-based constructs relatively straightforward, even if *Hind*III sites are unavailable for cloning and the cassettes have to be introduced into alternative sites after Klenow enzyme fill-in reaction and blunt-end ligation of vector and cassette (37). In addition, these cassettes enable the majority of mycobacterial DNA manipulations to be carried out in high-copy-number, general-purpose *E. coli* cloning vectors, which are not as functionally limited as existing mycobacterial plasmid shuttle vectors. Once the desired manipulation or analysis is completed for *E. coli*, insertion of a positive-selection integrase cassette into an available restric-

tion site is the only subcloning required to introduce the DNA into the mycobacterial chromosome. Integration of DNA into the chromosome of *M. intracellulare* facilitated by the integrase cassettes of pUC-HY-INT and pUC-GM-INT (Table 1) was highly stable in the absence of antibiotic selection and throughout in vivo passage in mice (tested for pUC-HY-INT only), correlating with the L5 integrase stability originally described for pMH94 in *M. smegmatis* and *M. tuberculosis* (26) and subsequently for pMH947 in *M. intracellulare* (27).

Gene disruption by insertion of antibiotic resistance markers may cause polar effects on neighboring loci and lead to alterations in phenotype which are unrelated to those solely due to the mutated gene. To control for such effects in our assessment of the growth of the 19Ag mutants in vivo, the mutants were complemented with a functional wild-type copy of the 19Ag gene by using the mycobacteriophage integrase cassettes. Although no significant growth differences were observed between the parental *M. intracellulare* strain (FM1) and the isogenic 19Ag mutant (EM32), after 35 days of mouse infection, the growth differential between strain EM32 and its derivatives carrying mycobacteriophage L5 integrants (both complemented mutant and vector control) was approximately 0.5 log (see Fig. 6B), a substantial difference in in vivo growth. These data suggest that no polar effects were associated with the 19Ag gene knockout strategy but may be associated with L5 vector insertion. Integration of L5 into the mycobacterial genome occurs via site-specific recombination between phage *attP* site and bacterial *attB* site, the core sequence of which overlaps a tRNA<sup>Gly</sup> gene at *attB* (33). The phenotypic consequences of DNA insertion at this site have not been fully determined; however, our study indicates that integrase-based vector insertion may impair the in vivo growth rate of *M. intracellulare*. If this finding holds true for other mycobacterial species, it may have important implications for studies aimed at complementing mycobacterial virulence or examining the contribution of specific genes using integrase-based cloning vectors.

Isolation of viable 19Ag gene mutants of *M. intracellulare* by site-directed mutagenesis demonstrated that the protein does not play an essential role in growth. The surface-associated lipoprotein antigens of mycobacteria have been suggested to be involved in nutrient binding and uptake, and a role in phosphate transport has been postulated for the *M. tuberculosis* 19Ag because its expression may be upregulated by phosphate starvation (2). We found that mutation of the 19Ag gene of *M. intracellulare* did not alter its ability to grow in phosphate-limited culture medium. Since the 38-kDa antigen of *M. intracellulare* has been shown to be homologous to the phosphate transport subunit S of the complex of proteins required for phosphate uptake in *E. coli* (42), the 19Ag may not play a major role in phosphate binding in this species. The growth rate of *M. intracellulare* on rich and minimal media was also unaffected by mutation of the 19Ag gene, also suggesting that it does not play an essential role in nutrient uptake. The occurrence of natural isolates of *M. tuberculosis* which lack expression of the 19Ag (25) also indicates that the protein is not essential for growth and pathogenesis of this mycobacterial species.

We here demonstrated that an isogenic 19Ag mutant of *M. intracellulare* was able to survive in mice and grow at the same rate as the parental strain, a strong indication that the 19Ag is not a virulence factor. However, in another report, Lathigra et al. (25) suggest that the 19Ag is indeed a virulence factor in *M. tuberculosis*, concluding this from the observation that a natural 19Ag mutant did not grow in mice as well as did another strain which produced the 19Ag. To support their contention, they complemented the 19Ag mutant with the

19Ag gene on a plasmid vector, which resulted in an improved survival of the complemented mutant within mouse spleen and lung compared to that of the mutant transformed with the vector alone. The authors rightly point out that their results do not unequivocally demonstrate a connection between virulence and the 19Ag because they were not working with isogenic strains (25). In addition, infection of mice with the complemented mutant resulted in higher bacterial counts only in the first and not the ninth week postinfection. This was attributed to the temporal loss of the recombinant plasmid in the absence of antibiotic selection within the mouse, though this contention was not substantiated by the use of integrative vectors. Other, equally possible explanations for this anomaly were not considered, however. No indication of bacterial uptake (day 1 counts) within the organs of the mice infected with the complemented mutant and the vector control were shown (25), presenting the possibility that the higher week 1 counts were due to differences in uptake of these two strains. Alternatively, as the mice were infected intraperitoneally and CFU numbers were assessed in the lungs and spleen, there is a requirement for seeding of the target organs from the peritoneal cavity. A difference in seeding rate between the two strains could have resulted in the observed difference at week 1. However, the most likely explanation for the enhanced survival of the complemented mutant in their model would be nonspecific effects of the vector because, over the same time period that the parental strain was rapidly eliminated from the spleen and lungs of infected mice, both the complemented mutant and the vector control strains survived and replicated (25).

Whereas the role of 19Ag in the virulence of *M. tuberculosis* remains unresolved, we have shown that the 19Ag is not a virulence factor in *M. intracellulare*. The absence of 19Ag in both avirulent (1403) and virulent (FM1) strains of *M. intracellulare* did not alter the growth kinetics of the bacteria in BALB/c mice. In addition, while the elimination of the avirulent strain 1403 could be substantially retarded by using immunocompromised SCID mice as hosts, the 19Ag mutant was not eliminated from these mice any more readily. Thus, site-directed mutagenesis of the 19Ag gene has unequivocally demonstrated that the antigen is not essential for the intracellular survival of *M. intracellulare*, and although we have not yet found a specific biological role for the protein, isolation of isogenic 19Ag mutants provides new tools for future functional studies.

#### ACKNOWLEDGMENTS

We thank Christiane Abou-Zeid for providing the purified rTB19Ag and William Jacobs for providing the cosmid vector pYUB412. We are indebted to Yossef Av-Gay for helpful discussion and comment.

This work was funded by research grants from the Action TB Initiative, Glaxo Wellcome, Canada, the Medical Research Council (MRC) of Canada/Pharmaceutical Manufacturers Association of Canada, and the Canadian Bacterial Disease Network. R.W.S. is a B.C. Lung Association/MRC scholar.

#### REFERENCES

1. Aldovini, A., R. N. Husson, and R. A. Young. 1993. The *uraA* locus and homologous recombination in *Mycobacterium bovis* BCG. *J. Bacteriol.* **175**: 7282-7289.
2. Andersen, A. B., and P. Brennan. 1994. Proteins and antigens of *Mycobacterium tuberculosis*, p. 307-332. B. R. Bloom (ed.), *In Tuberculosis: pathogenesis, protection, and control*. American Society for Microbiology, Washington, D.C.
3. Anonymous. 1972. Trudeau Mycobacterial Culture Collection catalog. National Institute for Allergy and Infectious Diseases, Bethesda, Md.
4. Ashbridge, K. R., R. J. Booth, J. D. Watson, and R. B. Lathigra. 1989. Nucleotide sequence of the 19kDa antigen from *Mycobacterium tuberculosis*. *Nucleic Acids Res.* **17**:1249.
5. Azad, A. K., T. D. Sirakova, L. M. Rogers, and P. E. Kolattukudy. 1996.



- Targeted replacement of the mycocerosic acid synthase gene in *Mycobacterium bovis* BCG produces a mutant that lacks mycosides. *Proc. Natl. Acad. Sci. USA* **93**:4787–4792.
6. Balasubramanian, V., M. S. Pavelka, Jr., S. S. Bardarov, J. Martin, T. R. Weisbrod, R. A. McAdam, B. R. Bloom, and W. R. Jacobs, Jr. 1996. Allelic exchange in *Mycobacterium tuberculosis* with long linear recombination substrates. *J. Bacteriol.* **178**:273–279.
  7. Baulard, A., L. Kremer, and C. Locht. 1996. Efficient homologous recombination in fast-growing and slow-growing mycobacteria. *J. Bacteriol.* **178**:3091–3098.
  8. Booth, R. J., D. L. Williams, K. D. Moudgil, L. C. Noonan, P. M. Grandison, J. J. McKee, R. L. Prestidge, and J. D. Watson. 1993. Homologs of *Mycobacterium leprae* 18-kilodalton and *Mycobacterium tuberculosis* 19-kilodalton antigens in other mycobacteria. *Infect. Immun.* **61**:1509–1515.
  9. Brooks, L. A. Chemical mutagenesis of mycobacteria. In T. Parish and N. Stoker (ed.), *Methods in molecular biology: mycobacteria protocols*, in press. The Humana Press Inc., Totowa, N.J.
  10. Collins, F. M., N. E. Morrison, and V. Montalbino. 1978. Immune response to persistent mycobacterial infection in mice. *Infect. Immun.* **20**:430–438.
  11. Collins, F. M., and R. W. Stokes. 1987. *Mycobacterium avium*-complex infections in normal and immunodeficient mice. *Tubercle* **68**:127–136.
  12. Collins, F. M., and S. R. Watson. 1981. Immune responses to atypical mycobacterial lung infections. *Rev. Infect. Dis.* **3**:981–989.
  13. Collins, M., A. Paiki, S. Wahl, A. Nolan, J. Goodger, M. Woodward, and J. W. Dale. 1990. Cloning and characterization of the gene for the 19kDa antigen of *Mycobacterium bovis*. *J. Gen. Microbiol.* **136**:1429–1436.
  14. Dunbar, F. P., I. Pejovic, R. Cacciatore, L. Peric-Golia, and E. H. Runyon. 1968. *Mycobacterium intracellulare* maintenance of pathogenicity in relationship to lyophilization and colony form. *Scand. J. Respir. Dis.* **49**:153–162.
  15. Falkinham, J. O. 1996. Epidemiology of infection by nontuberculous mycobacteria. *Clin. Microbiol. Rev.* **9**:177–215.
  16. Garbe, T., D. Harris, M. Vordermeier, R. Lathigra, J. Ivanyi, and D. Young. 1993. Expression of the *Mycobacterium tuberculosis* 19-kilodalton antigen in *Mycobacterium smegmatis*: immunological analysis and evidence of glycosylation. *Infect. Immun.* **61**:260–267.
  17. Hänsch, H. C. R., D. A. Smith, M. E. A. Mielke, H. Hahn, G. J. Bancroft, and S. Ehlers. 1996. Mechanisms of granuloma formation in murine *Mycobacterium avium* infection: the contribution of CD4+ T cells. *Int. Immunol.* **8**:1299–1310.
  18. Harlow, E., and D. Lane (ed.). 1988. *Antibodies: a laboratory manual*. Cold Spring Harbor Laboratory Press, Cold Spring Harbor, N.Y.
  19. Harris, D. P., H.-M. Vordermeier, S. J. Brett, G. Pasvol, C. Moreno, and J. Ivanyi. 1994. Epitope specificity and isoforms of the mycobacterial 19-kilodalton antigen. *Infect. Immun.* **62**:2963–2972.
  20. Herrmann, J. L., P. O'Gaora, A. Gallagher, J. E. Thole, and D. B. Young. 1996. Bacterial glycoproteins: a link between glycosylation and proteolytic cleavage of a 19 kDa antigen from *Mycobacterium tuberculosis*. *EMBO J.* **15**:3547–3554.
  21. Husson, R. N., B. E. James, and R. A. Young. 1990. Gene replacement and expression of foreign DNA in mycobacteria. *J. Bacteriol.* **172**:519–524.
  22. Inderleid, C. B., C. A. Kemper, and L. E. M. Bermudez. 1993. The *Mycobacterium avium* complex. *Clin. Microbiol. Rev.* **6**:266–310.
  23. Ivanyi, J., and J. E. Thole. 1994. Specificity and function of T and B cell recognition in tuberculosis, p. 437–458. In B. R. Bloom (ed.), *Tuberculosis: pathogenesis, protection, and control*. American Society for Microbiology, Washington, D.C.
  24. Kalpana, G. V., B. R. Bloom, and W. R. Jacobs, Jr. 1991. Insertional mutagenesis and illegitimate recombination in mycobacteria. *Proc. Natl. Acad. Sci. USA* **88**:5433–5437.
  25. Lathigra, R., Y. Zhang, M. Hill, M. J. Garcia, P. S. Jactett and J. Ivanyi. 1996. Lack of production of the 19-kDa glycolipoprotein in certain strains of *Mycobacterium tuberculosis*. *Res. Microbiol.* **147**:237–249.
  26. Lee, M. H., L. Pascopella, W. R. Jacobs, Jr., and G. F. Hatfull. 1991. Site-specific integration of mycobacteriophage L5: integration-proficient vectors for *Mycobacterium smegmatis*, *Mycobacterium tuberculosis*, and bacille Calmette-Guerin. *Proc. Natl. Acad. Sci. USA* **88**:3111–3115.
  27. Marklund, B.-I., D. P. Speert, and R. W. Stokes. 1995. Gene replacement through homologous recombination in *Mycobacterium intracellulare*. *J. Bacteriol.* **177**:6100–6105.
  - 27a. Marklund, B.-I., and R. W. Stokes. Unpublished data.
  28. McFadden, J. 1996. Recombination in mycobacteria. *Mol. Microbiol.* **21**:205–211.
  29. Nair, J., D. A. Rouse, and S. L. Morris. 1992. Nucleotide sequence analysis and serologic characterization of the *Mycobacterium intracellulare* homologue of the *Mycobacterium tuberculosis* 19kDa antigen. *Mol. Microbiol.* **6**:1431–1439.
  30. Norman, E., O. A. Dellagostin, J. McFadden, and J. W. Dale. 1995. Gene replacement by homologous recombination in *Mycobacterium bovis* BCG. *Mol. Microbiol.* **16**:755–760.
  31. Pavelka, M. S., Jr., and W. R. Jacobs, Jr. 1996. Biosynthesis of diaminopimelate, the precursor of lysine and a component of peptidoglycan, is an essential function of *Mycobacterium smegmatis*. *J. Bacteriol.* **178**:6496–6507.
  32. Pelicic, V., J. M. Reytrat, and B. Gicquel. 1996. Positive selection of allelic exchange mutants in *Mycobacterium bovis* BCG. *FEMS Microbiol. Lett.* **144**:161–166.
  33. Pena, C. E., J. E. Stoner, and G. F. Hatfull. 1996. Positions of strand exchange in mycobacteriophage L5 integration and characterization of the attB site. *J. Bacteriol.* **178**:5533–5536.
  34. Prestidge, R. L., P. M. Grandison, D. W. Chuk, R. J. Booth, and J. D. Watson. 1995. Production of the 19-kDa antigen of *Mycobacterium tuberculosis* in *Escherichia coli* and its purification. *Gene* **164**:129–132.
  35. Reytrat, J. M., F. X. Berthet, and B. Gicquel. 1995. The urease locus of *Mycobacterium tuberculosis* and its utilization for the demonstration of allelic exchange in *Mycobacterium bovis* bacillus Calmette-Guerin. *Proc. Natl. Acad. Sci. USA* **92**:8768–8772.
  36. Reytrat, J. M., G. Lopez-Ramirez, C. Ofredo, B. Gicquel, and N. Winter. 1996. Urease activity does not contribute dramatically to persistence of *Mycobacterium bovis* bacillus Calmette-Guerin. *Infect. Immun.* **64**:3934–3936.
  37. Sambrook, J., E. F. Fritsch, and T. Maniatis. 1989. *Molecular cloning: a laboratory manual*, 2nd ed. Cold Spring Harbor Laboratory Press, Cold Spring Harbor, N.Y.
  38. Sander, P., A. Meier, and E. C. Bottger. 1995. rpsL+: a dominant selectable marker for gene replacement in mycobacteria. *Mol. Microbiol.* **16**:991–1000.
  39. Schaefer, W. B., C. L. Davis, and M. L. Cohn. 1970. Pathogenicity of transparent, opaque, and rough variants of *Mycobacterium avium* in chickens and mice. *Am. Rev. Respir. Dis.* **102**:499–506.
  40. Schweizer, H. D. 1993. Small broad-host-range gentamycin resistance gene cassette for site specific insertion and deletion mutagenesis. *BioTechniques* **15**:831–834.
  41. Snapper, S. B., R. E. Melton, S. Mustafa, T. Kieser, and W. R. Jacobs, Jr. 1990. Isolation and characterization of efficient plasmid transformation mutants of *Mycobacterium smegmatis*. *Mol. Microbiol.* **4**:1911–1919.
  42. Thangaraj, H. S., T. J. Bull, K. A. L. De Smet, M. K. Hill, D. A. Rouse, C. Moreno, and J. Ivanyi. 1996. Duplication of the genes encoding the immunodominant 38 kDa antigen in *Mycobacterium intracellulare*. *FEMS Microbiol. Lett.* **144**:235–240.
  43. Young, D. B., and T. R. Garbe. 1991. Lipoprotein antigens of *Mycobacterium tuberculosis*. *Res. Microbiol.* **142**:55–65.
  44. Young, D. B., S. H. Kaufmann, P. W. Hermans, and J. E. Thole. 1992. Mycobacterial protein antigens: a compilation. *Mol. Microbiol.* **6**:133–145.
  45. Young, D. B., and K. Duncan. 1995. Prospects for new interventions in the treatment and prevention of mycobacterial disease. *Annu. Rev. Microbiol.* **49**:642–673.
  46. Zalacain, M., A. Gonzalez, M. C. Guerrero, R. J. Mattaliano, F. Malpartida, and A. Jimenez. 1986. Nucleotide sequence of the hygromycin B phosphotransferase gene from *Streptomyces hygroscopicus*. *Nucleic Acids Res.* **14**:1565–1581.